Sub-Doppler spectroscopy using a multiple-reflection mirror system

Yit-Tsong Chen, Joan M. Frye,* and Takeshi Oka

Department of Chemistry, The University of Chicago, Chicago, Illinois 60637

Received January 6, 1986; accepted March 3, 1986

A sub-Doppler spectroscopic technique using a Fresnel rhomb is combined with the White multiple-reflection cell to increase the sensitivity of ultrahigh-resolution spectroscopy. Microwave sidebands on CO_2 laser radiation have been used as a frequency-tunable infrared source with high spectral purity. A gain of 4–8 in the path length with a resolution of ~100 kHz has been readily obtained. Applications of this method to observation of the hyperfine structure of NH_3 and PH_3, the K doubling of PH_3, and the Stark spectrum of PH_3 and SiH_4 are given.

INTRODUCTION

One of the most powerful spectroscopic techniques to achieve sub-Doppler resolution is the inverse Lamb dip method in which molecules interact with two counterpropagating laser radiation beams.[1] The simplest way to make such an optical arrangement is to reflect the laser beam (which has passed through the sample cell) back into the cell with a mirror. The reflected beam nearly coincides with the incoming beam but is slightly shifted so that it can be sent into a detector without interfering with the incoming beam. The incomplete collimation of the two counterpropagating beams results in a loss of sensitivity and resolution. This can be avoided by use of a $\lambda/4$ plate[2] or a Fresnel rhomb,[3] which will make the two counterpropagating radiations completely collimated. After passing through such an element, the originally plane-polarized laser radiation is circularly polarized. Then, after the radiation is reflected from the mirror and goes through the element again, it is again linearly polarized, but with the plane of polarization perpendicular to that of the incoming beam. Thus the two beams can be separated by a Brewster-angle window. This optical arrangement not only increases the sensitivity and resolution but also allows for a more sophisticated optical setup for spectroscopy because the two well-collimated counterpropagating beams can be maneuvered like a single beam. In this paper we report our results of combining this technique with the well-known multiple-reflection method using a White cell arrangement.[4] We have found that an increase of 4–8 in the optical path length is quite straightforward. We think that this method is promising for high-sensitivity sub-Doppler spectroscopy for low-concentration transient species, such as molecular ions and free radicals. In this paper we summarize our results for the simpler molecules NH_3, PH_3, and SiH_4.

EXPERIMENT

We used microwave sidebands on CO_2 laser radiation as the frequency-tunable coherent infrared radiation source for sub-Doppler spectroscpy (Fig. 1). Infrared radiation with frequency ν_1 of ~3 W from a CO_2 laser and microwave radiation with frequency ν_m of ~20 W are mixed in CdTe crystal.[5,6] This generates microwave sidebands on CO_2 laser radiation with frequency $\nu_1 \pm \nu_m$ with a power of ~1 mW and spectral purity of ~20 kHz. The planes of polarization for the carrier and the sidebands are perpendicular to each other. A part of the CO_2 radiation is reflected by a Brewster-angle window and directed to a CO_2 fluorescence cell for stabilization. The frequency of the CO_2 laser radiation is Doppler modulated by a vibrating reflection mirror mounted on a speaker.[7]

The sideband radiation used for spectroscopy passes through a Fresnel rhomb of ZnSe and is circularly polarized as it is directed into the White cell. The multiple-reflection mirrors are 2 cm in diameter with a radius of curvature of 2.4 m. The 2.5-m cell contains a pair of Stark plates separated by 1 cm for the observation of the Stark effect. After 4–8 traversals the radiation leaves the multiple-reflection mirror system in the usual way. At the exit of the system a plane mirror was placed and was adjusted carefully so that the reflected beam was exactly collimated with the incident beam. Thus the circularly polarized radiation retraces its optical path, leaves the multiple-reflection system, and returns to the Fresnel rhomb. After passing the Fresnel rhomb, the outgoing beam, which now has a plane of polarization perpendicular to that of the incoming beam, is reflected by the Brewster-angle window and sent into a 1-m grating monochromator. The monochromator passes only one of the two sidebands used for spectroscopy; it also reduces the carrier CO_2 radiation. A grid polarizer, which is placed in front of the detector, further reduces the strong CO_2 carrier entering the signal channel.

In order to increase the sensitivity, the frequency of the sidebands is modulated by the frequency modulation of the microwave radiation (modulation frequency 10 kHz, depth ~ 50 kHz), and the sharp sub-Doppler dip signals are processed through a phase-sensitive detector.

The presence of the sample was typically ~3 m Torr, which was measured by a capacitance manometer. With this arrangement the following broadenings are expected:

pressure broadening ~ 60 kHz,
transit broadening ~ 10 kHz,
power broadening ~ 50 kHz.

0740-3224/86/070935-05$02.00

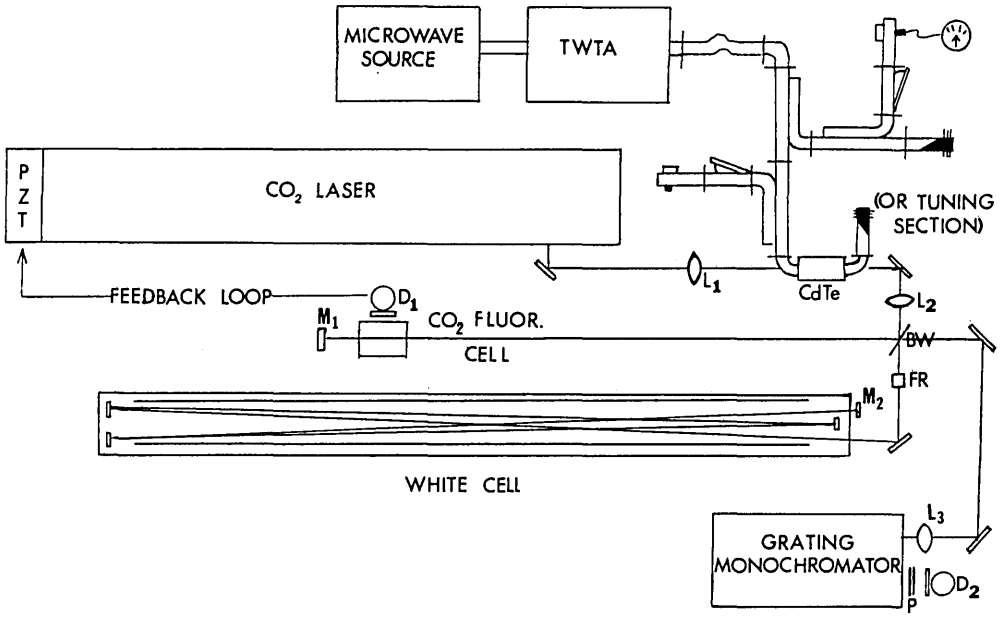

Fig. 1. Experimental setup. L_1–L_3, ZnSe lenses; M_1, reflection mirror mounted on a speaker; M_2, plane reflection mirror; D_1, InSb detector; D_2, HgCdTe detector; BW, Brewster-angle window; FR, Fresnel rhomb; P, grid polarizer; TWTA, traveling-wave tube amplifier; PZT, piezoelectric translator.

OBSERVED RESULTS

Hyperfine Structure in NH_3 ν_2 Band

The observed ^{14}N nuclear quadrupole hyperfine structure for the $as^qP(1, 0)$ transition is shown in Fig. 2. The energy-level diagram for the transitions is shown below, in which transitions for the normal Lamb dip and crossover double-resonance dips are indicated. Compared with earlier work,[8] here the features are much better resolved and the signal-to-noise ratio higher. In this case, the observed hyperfine structure is due solely to hyperfine structure in the ground state.

The observed hyperfine structure for the $as^qQ(4, 4)$ transition of $^{14}NH_3$ and the energy-level system are shown in Fig. 3. In this case both the upper state and the lower state have hyperfine splittings. The strong central feature corresponds to the three overlapped $\Delta F = 0$ transitions, which under higher resolution are just split as shown in the second trace with magnification. This is because of the small difference of eqQ in the ν_2 and the ground states. The separation between the $F = 4 \leftarrow 4$ transition and the other two $\Delta F = 0$ transitions ($3 \leftarrow 3$ and $5 \leftarrow 5$) was observed to be ~95 kHz. The four $\Delta F = \pm 1$ transitions are expected to be ~50 times weaker and were not observed directly as saturation dips. However, the crossover dips between them and the strong $\Delta F = 0$ transitions are detected as four satellites. Thus the positions of the $\Delta F = \pm 1$ transitions can be located from the frequencies of the crossover dips.

K Doubling, Hyperfine Structure, and Stark Splitting in PH_3

The $K = 3n$ rotational levels in the nondegenerate vibrational modes of a C_{3v} symmetric-top molecule, such as PH_3, split into the A_1–A_2 doublet because of high-order centrifugal distortion. Figure 4 shows such a splitting in the $^qP(6, 3)$ ν_2 transition of PH_3 and the associated energy-level system. Using the previously reported value for the ground-state splitting of PH_3,[9] we determined the K doubling for the ν_2 =

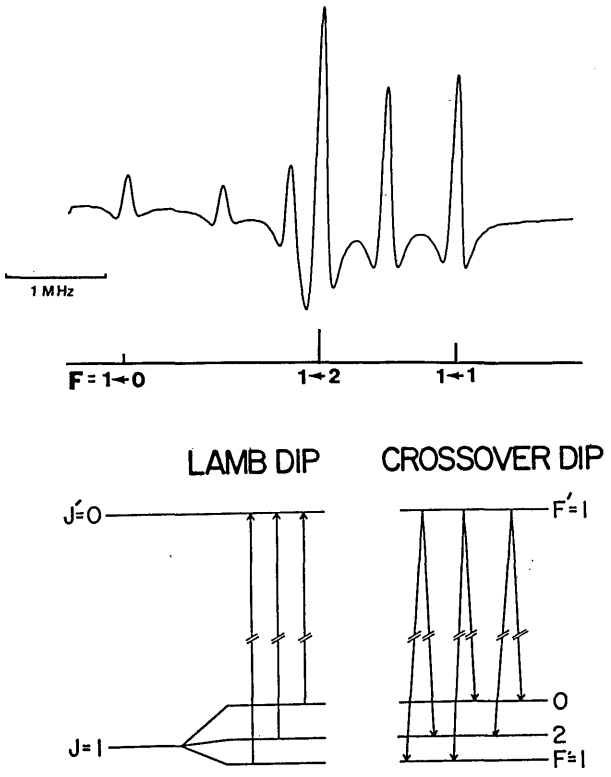

Fig. 2. Observed ^{14}N nuclear quadrupole hyperfine structure for the $as^qP(1, 0)$ transition in the ν_2 band of NH_3 and the energy-level diagram. The three hyperfine components ($\Delta F = 1 \leftarrow 0, 1 \leftarrow 1, 1 \leftarrow 2$) and the three crossover dips are clearly resolved. The energy-level diagram for the inverse Lamb dips and for the crossover double-resonance dips are shown below. The upper microwave sideband of the CO_2 $10P(16)$ laser line with $\nu_m \sim 14\,690$ MHz was used. The gas pressure of the sample was ~3 mTorr, and the time constant of detection was 125 msec.

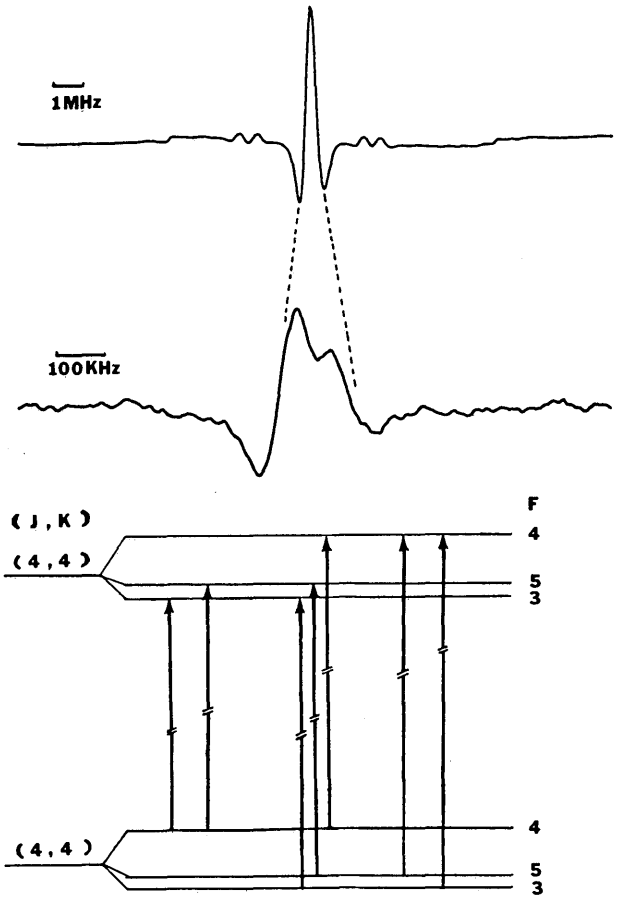

Fig. 3. Observed hyperfine structure and energy-level diagram for the $as^qQ(4, 4)$ transition of NH_3. The strong central feature corresponds to the three overlapped $\Delta F = 0$ transitions that under higher resolution are just split because of the small difference of eqQ in the ν_2 and the ground state. The weak $\Delta F = \pm 1$ transitions were not observed as Lamb dips owing to insufficient saturation, but the center dips between them and the $\Delta F = 0$ transitions are clearly seen as four satellites. The lower microwave sideband of the CO_2 $10R(6)$ laser line with $\nu_m \sim 16\,930$ MHz was used. The gas pressure was ~3 mTorr, and the time constant was 125 msec for the top trace and 400 msec for the bottom trace. The frequency increases from right to left.

1, $J = 5$, $k = 3$ state to be 13.22 MHz. This is much greater than the value for the ground state and shows that the high-order centrifugal distortion varies greatly with the vibrational excited state.

Figure 5 shows a high-resolution spectrum of PH_3 and the energy-level system in which the small magnetic spin-rotation hyperfine structure due to the ^{31}P nucleus is studied. The $F = 1/2 \leftarrow 3/2$ and $F = 3/2 \leftarrow 5/2$ transitions separated by ~110 kHz are barely resolved. The observed splittings showed that the value of the spin-rotation constants in the ν_2 state of PH_3 is similar to that of the ground state. The other weaker infrared transition $F = 3/2 \leftarrow 3/2$, however, was not observed because of the insufficient saturation.

In Fig. 6 the Lamb-dip Stark spectrum of the $^qR(8, 1)$ ν_2 transition of PH_3 at $E = 1000$ V/cm is shown. The circularly polarized radiation in the sample cell gives rise to the transitions with $\Delta M = 0, \pm 1$ selection rules. The small difference of the dipole moments between the ν_2 state and the ground state made various $\Delta M = 0, \pm 1$ transitions overlap. The weaker features in the middle of saturation dips are due to

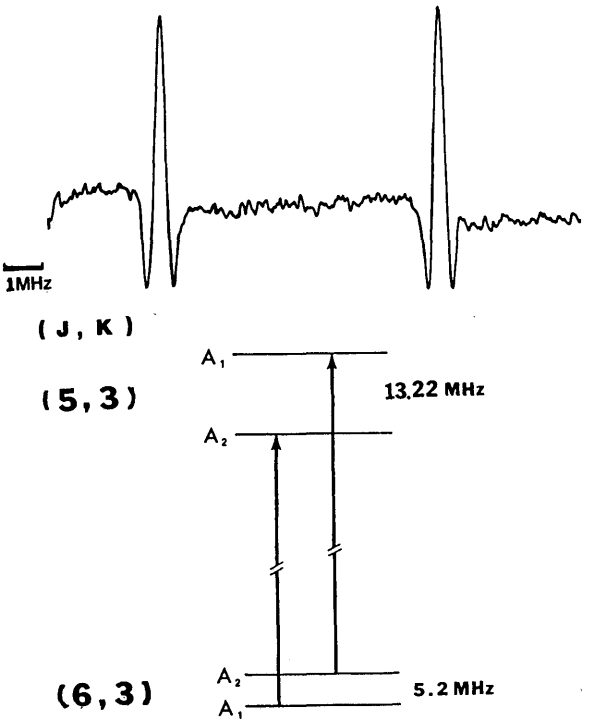

Fig. 4. Observed K-type doubling of the $^qP(6, 3)$ ν_2 transition of PH_3. The measurement shows that the K doubling in the ν_2 state (13.22 MHz) is much larger than that of the corresponding ground state (1.7 MHz). The upper microwave sideband of the CO_2 $10P(30)$ laser line with $\nu_m \sim 14\,660$ MHz was used. The PH_3 pressure was 5 mTorr, and the time constant of detection was 125 msec. The frequency increases from right to left.

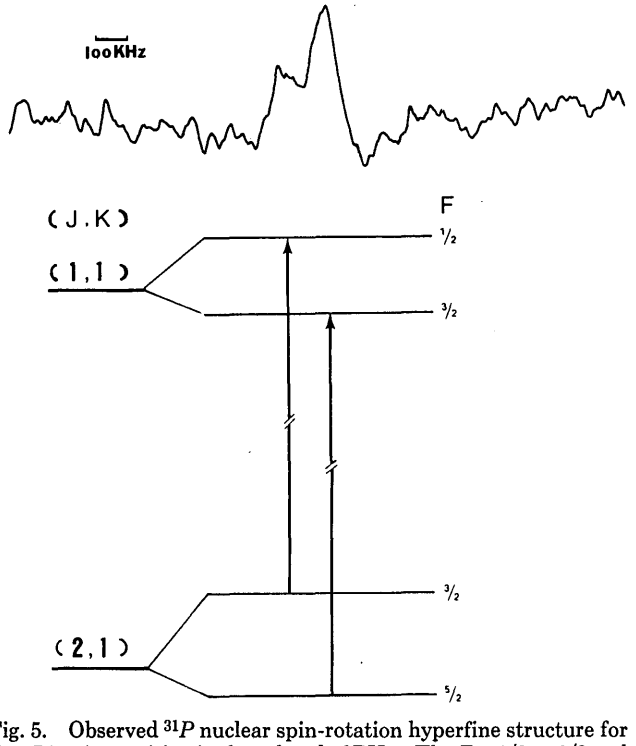

Fig. 5. Observed ^{31}P nuclear spin-rotation hyperfine structure for the $^qP(2, 1)$ transition in the ν_2 band of PH_3. The $F = 1/2 \leftarrow 3/2$ and $F = 3/2 \leftarrow 5/2$ components are barely resolved. The $F = 3/2 \leftarrow 3/2$ component was not observed as a saturation dip owing to its weaker intensity (1/4). The lower microwave sideband of the CO_2 $10R(18)$ laser line with $\nu_m \sim 13\,390$ MHz was used. The gas pressure was ~4 mTorr, and the time constant was 400 msec. The frequency increases from right to left.

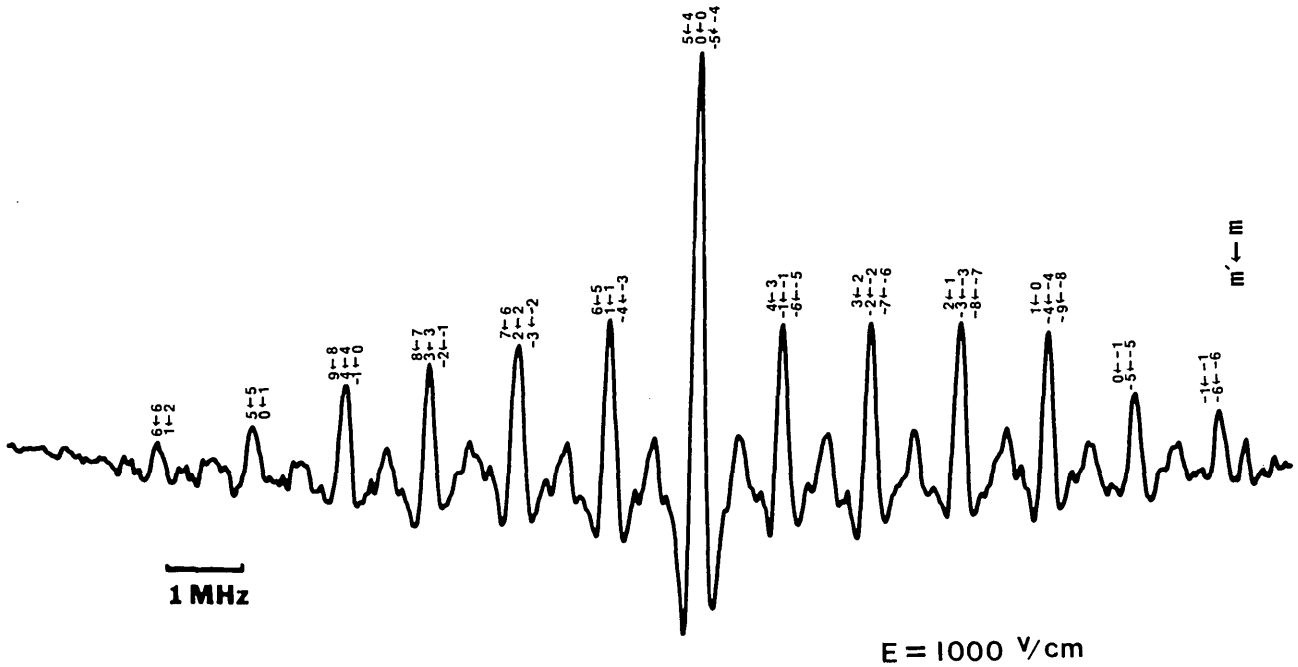

Fig. 6. Observed Lamb-dip Stark spectrum of the $^qR(8, 1)$ ν_2 transition of PH_3 at $E = 1000$ V/cm. The circularly polarized radiation in the sample cell gives rise to the transitions with $\Delta M = 0, \pm 1$ selection rules. Because of the small difference between the dipole moments of the ground and of the ν_2 states, each peak is composed of the overlapped $\Delta M = 0, \pm 1$ transitions with the magnetic quantum numbers m for the ground state and m' for the ν_2 state. The weak features between the inverse Lamb dips are the collision-induced center dips. The upper microwave sideband of the CO_2 9P(8) laser line with $\nu_m \sim 14\,965$ MHz was used. The gas pressure was 5 mTorr, and the time constant was 125 msec.

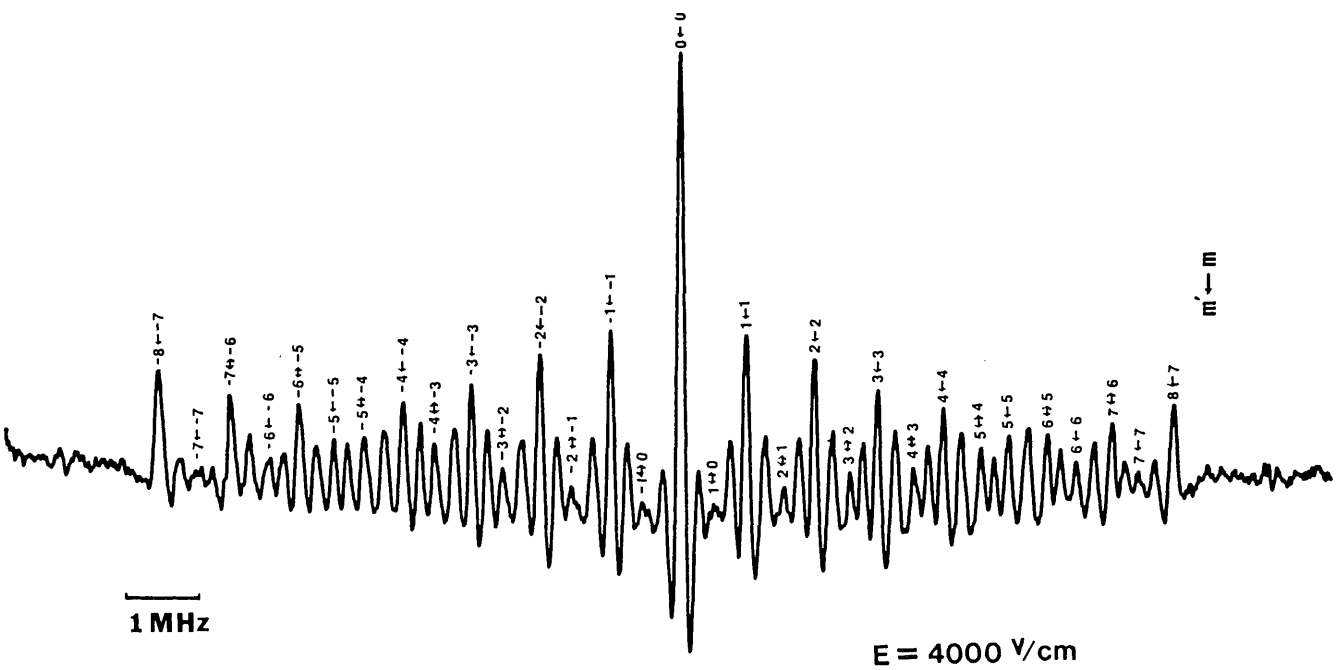

Fig. 7. Observed Lamb-dip Stark spectrum of the $R(7)E$ ν_4 transition of SiH_4 at $E = 4000$ V/cm. The $\Delta M = 0$ inverse Lamb dips were resolved from those of $\Delta M = \pm 1$ and the crossover dips located between the two corresponding inverse Lamb dips. In addition to the vibration-induced dipole moment of $1.46(5) \times 10^{-2}$ D, the centrifugal distortion produces a dipole moment with the Watson coefficient of $2.97(19) \times 10^{-5}$ D. The lower microwave sideband of the CO_2 10P(34) laser line with $\nu_m \sim 16\,910$ MHz was used. The gas pressure was 5 mTorr, and the time constant was 300 msec.

collision-induced center dips.[10] They are of particular interest for studying rotational inelastic collisions and the variation of molecular velocity accompanying the collisions.

Vibration-Induced Dipole Moment in SiH_4

The E rovibrational levels of the SiH_4 molecule exhibit a first-order Stark effect due to a vibration-induced dipole

moment[11] if the molecule is in a triply degenerate state.[12,13] In Fig. 7, the observed Lamb-dip Stark spectrum of the $R(7)E$ ν_4 transition of SiH_4 at $E = 4000$ V/cm is shown. The $\Delta M = 0$ lines were resolved from the $\Delta M = \pm 1$ lines; between the inverse Lamb dips are the crossover dips. The centrifugal distortion-induced dipole moment and the vibration-induced dipole moment in the ν_4 state were determined independently from these measurements. The vibration-induced dipole moment, which is $\sim\kappa^2$ (κ is the Born–Oppenheimer constant) smaller than a typical permanent dipole moment, was determined to be $1.46(5) \times 10^{-2}$ D. The induced dipole moment contributed from the centrifugal distortion is $2.97(19) \times 10^{-5}$ D.

SUMMARY

We have shown that, by using a Fresnel rhomb or a $\lambda/4$ plate, we can combine the high resolution of sub-Doppler spectroscopy and the high sensitivity of a multiple-reflection White cell. We believe that this method can be used effectively for the ultrahigh-resolution spectrum of transient species, such as molecular ions and free radicals.

ACKNOWLEDGMENTS

We thank G. Magerl for earlier discussions on this problem. This work was supported in part by the Louis Block Fund of The University of Chicago. J. M. Frye thanks the National Organization of Black Chemists and Chemical Engineers and the Eastman Kodak Company for postdoctoral support. We thank T. Frye for providing the computer hardware and software necessary to drive the microwave synthesizer sweeper.

The authors are also with the Department of Astronomy and Astrophysics, The University of Chicago.

* Present address, Institut für Nachrichtentechnik, Technische Universität Wien, Gusshausstrasse 25, A-1040 Wien, Austria.

REFERENCES

1. P. H. Lee and M. L. Skolnick, Appl. Phys. Lett. **10,** 303 (1967); R. L. Barger and J. L. Hall, Phys. Rev. Lett. **22,** 4 (1969).
2. J. L. Hall and C. J. Borde, Phys. Rev. Lett. **30,** 1101 (1973).
3. M. Born and E. Wolf, *Principles of Optics* (Pergamon, London, 1980).
4. J. U. White, J. Opt. Soc. Am. **32,** 285 (1942).
5. G. Magerl, W. Schupita, and E. Bonek, IEEE J. Quantum Electron. **QE-18,** 1214 (1982).
6. G. Magerl, J. M. Frye, W. A. Kreiner, and T. Oka, Appl. Phys. Lett. **42,** 656 (1982).
7. W. Schupita, A. Ullrich and G. Magerl, Technical University of Vienna, Vienna, Austria (personal communication).
8. G. Magerl, W. Schupita, J. M. Frye, W. Kreiner, and T. Oka, J. Mol. Spectrosc. **107,** 72 (1984).
9. P. B. Davis, R. M. Neumann, S. C. Wofsy, and W. Klemperer, J. Chem. Phys. **55,** 3654 (1971).
10. J. W. C. Johns, A. R. W. McKellar, T. Oka, and M. Romheld, J. Chem. Phys. **62,** 1488 (1975).
11. M. Mizushima and P. Venkateswarlu, J. Chem. Phys. **21,** 705 (1953).
12. I. M. Mills, J. K. G. Watson, and W. L. Smith, Mol. Phys. **16,** 329 (1969).
13. J. K. G. Watson, J. Mol. Spectrosc. **50,** 281 (1974).